The stability of the rhombohedral α-Hg phase alloyed with Sn under high pressure up to 30 GPa

2003 J. Phys.: Condens. Matter 15 7489

(http://iopscience.iop.org/0953-8984/15/44/005)

INSTITUTE OF PHYSICS PUBLISHING JOURNAL OF PHYSICS: CONDENSED MATTER

J. Phys.: Condens. Matter **15** (2003) 7489–7500 PII: S0953-8984(03)66873-6

The stability of the rhombohedral α-Hg phase alloyed with Sn under high pressure up to 30 GPa

V F Degtyareva[1], I K Bdikin[1], F Porsch[2] and N I Novokhatskaya[1]

[1] Institute of Solid State Physics, Russian Academy of Sciences, Chernogolovka, Moscow District, 142432, Russia
[2] Mineralogisch-Petrologisches Institut, Universität-Bonn, 53113 Bonn, Germany

Received 29 July 2003, in final form 30 September 2003
Published 24 October 2003
Online at stacks.iop.org/JPhysCM/15/7489

Abstract

The effects of pressure on phase stability of an HgSn alloy with nearly equiatomic composition have been studied up to 30 GPa with diamond anvil cells using x-ray powder diffraction with synchrotron radiation. A Hg-rich phase *hR*1-(Hg) with a rhombohedral distortion of a face-centred cubic (fcc) cell is found to form in the alloy at pressures above 3 GPa in coexistence with a Sn-rich phase with a simple hexagonal structure sh-*hP*1 stable at ambient pressure. While the sh-*hP*1 phase transforms at pressures above 15 GPa to a body-centred tetragonal bct-*tI*2 phase, the *hR*1-(Hg) phase remains stable up to 30 GPa. The *hR*1-(Hg) phase is regarded as a solid solution of Sn in α-Hg. The range of solubility is estimated from about 5 to 10 at.% Sn. The alloying of Hg with Sn stabilises the α-Hg phase up to pressure of 30 GPa, while pure α-Hg becomes unstable at 3.7 GPa transforming to a bct (*tI*2) phase. The *hR*1-(Hg) phase reveals a strong anisotropy on compression. An increase of c/a from 1.99 to 2.25 in the pressure range from 2.6 to 29.9 GPa is observed displaying a trend towards fcc with $c/a = 2.45$ in a primitive rhombohedral setting (hexagonal axes).

The stabilisation of the *hR*1-(Hg) phase by alloying with Sn and the range of solubility of Sn in α-Hg are discussed within the concept of Fermi sphere–Brillouin zone interactions.

1. Introduction

Binary alloy systems display under pressure the evolution of phase equilibria including the following effects [1–3]:

(i) extension of solid solutions based on metallic type phases of components stable at ambient or high pressure;
(ii) destabilization of intermediate phases or compounds of low-coordinated structures and of stoichiometric compositions;

(iii) formation of new intermediate high pressure phases of high-coordinated structures with metallic type bonding.

Of special interest are binary alloy systems of sp elements adjacent in the periodic table which have small differences in atomic size and electronegativity. High-pressure studies of these alloys allow the determination of the factors of phase formation and stability primarily related to the mean number of valence electrons per atom, i.e. the electron concentration z. One of the interesting systems in this respect is the Hg–Sn system, because both components represent s or sp metals with nearly equal atomic radii of 1.57 and 1.55 Å, respectively, [4].

The elements Hg and Sn display under pressure a number of structural transitions. The following phase transition sequences are found.

Sn : β-Sn, bct-$tI4$($<$9.5 GPa) $\rightarrow$ bct-$tI2$($<$45 GPa) $\rightarrow$ bcc [5];

Hg : α-Hg, $hR1$($<$3.7 GPa) $\rightarrow$ β-Hg, bct-$tI2$($<$12 GPa)
$\rightarrow$ $oP4$($\lesssim$38 GPa) $\rightarrow$ hcp [6, 7].

These elements have a common high-pressure structure bct-$tI2$ in the pressure range from 9 to 12 GPa. As the atomic radii in these elements are similar one can expect an extended region of solubility in this system under pressure, in accordance with the known Hume-Rothery rule.

In the Hg–Sn system at ambient condition, the Sn and Hg solid solutions are of very limited extent (less than 0.5 at.%), and one intermediate Sn-rich phase is known with the composition range from 6 to 12 at.% Hg [8]. This intermediate phase ($HgSn_9$) has a simple hexagonal structure, $hP1$, space group $P6/mmm$ [9]. Under pressure a transition from the $hP1$ phase to a body-centred tetragonal phase, bct-$tI2$, space group $I4/mmm$, has been observed in the alloy $Hg_{10}Sn_{90}$ [10]. The bct-$tI2$ phase is considered as a solid solution on the base of bct-$tI2$ high-pressure phase of Sn-II. To study the possible extension of the bct-Sn solid solution to higher Hg content, an alloy $Hg_{15}Sn_{85}$ was later investigated [3]. Transformation of the $hP1$ phase to the bct-$tI2$ phase was found [3] in accordance with the previous study [10]. However, an additional phase of higher Hg content was observed in this alloy under pressure with a structure preliminary described as an In-type tetragonal distortion of a face-centred cubic (fcc) structure. To accurately determine the structure of this new intermediate phase, it is therefore necessary to study Sn–Hg alloys with higher Hg content.

In the present paper the results of high-pressure studies of an $Hg_{50}Sn_{50}$ alloy with nearly equiatomic composition are presented. An Hg-rich phase is observed in the pressure range from $\sim$3 GPa up to at least 30 GPa. The crystal structure of this phase is identified as a rhombohedrally distorted fcc structure related to the α-Hg structure and is considered as a solid solution of Sn in the α-Hg phase.

2. Experimental details

The alloy $Hg_{50}Sn_{50}$ (of equiatomic composition) was prepared by melting the appropriate amounts of the pure elements (5N purity). Alloy components were heated up to 500 °C in a quartz tube under inert gas atmosphere and cooled down rapidly to room temperature. At ambient conditions the alloy consists of a mixture of liquid Hg and an intermediate $HgSn_9$ phase with the simple hexagonal structure. The sample loaded into the high-pressure cell was a mixture of solid particles of this phase and the Hg-rich liquid. In this case it is difficult to control precisely the content of the sample composition and a slight deviation from the composition of the bulk alloy is possible. However, in this study there were four separate runs with different sample loading, and similar results were obtained. Therefore the sample composition in all cases is assumed to be close to that of the bulk alloys and is further referred

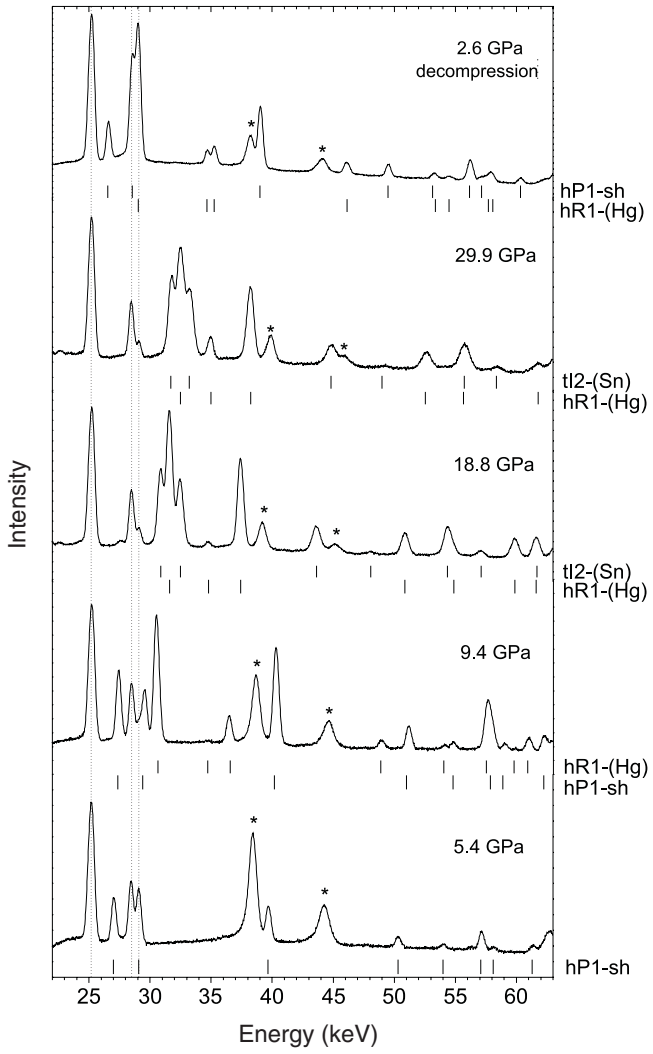

Figure 1. Selected energy-dispersive diffraction spectra of the HgSn alloy collected under different pressures with $2\theta = 9.03°$ ($Ed = 7875$ keV pm). Fluorescence peaks from Sn are marked by vertical dotted lines. The tick marks below the spectra show the calculated peak positions for each phase indicated on the right side. For the spectrum at 5.4 GPa there is a mixture of the crystalline sh-$hP1$ phase and a liquid Hg-rich phase. The lattice parameters of the phases are listed in table 1. Stars denote diffraction peaks from the gasket material (inconel).

to as HgSn. Evaluation of the experimental data obtained under pressure provided evidence for the sample composition to be close to equiatomic (see section 3).

High-pressure studies were performed with diamond anvil cells [11] and energy-dispersive diffraction using synchrotron radiation at DESY, HASYLAB [12, 13]. The ruby luminescence technique [14] was used for pressure measurements with the non-linear ruby scale [15]. The alloy samples were loaded into the gasket hole with diameter 200 μm after pre-indentation of the gasket from 400 to $\sim$80 μm. Experiments were performed without any pressure-transmitting medium because the sample contains liquid phase initially and is a quite soft solid at high pressure. Exposure time was typically 10–15 min and $\sim$1 h for principal patterns. The

Table 1. Structural characteristic of phases in the HgSn alloy at different pressures.

Pressure (GPa)	Phase	Lattice parameters (pm) a	c	c/a	V_{at} (10^6 pm^3)
2.6 (unload)	*hP*1-sh	318.2(1)	296.4(6)	0.931	26.00
	*hR*1-(Hg) (hexagonal cell)	341.7(1)	681.5(4)	1.994	22.97
29.9	bct-Sn	351.5(1)	321.3(2)	0.914	19.85
	*hR*1-(Hg)	299.7(2)	674.4(9)	2.250	17.48
18.8	bct-Sn	361.4(1)	327.9(1)	0.907	21.41
	*hR*1-(Hg)	309.73(5)	679.8 (3)	2.195	18.83
9.4	*hR*1-(Hg)	322.10(3)	682.96(1)	2.12	20.46
	*hP*1-sh	309.0(5)	287.5(4)	0.930	23.76
5.4	*hP*1-sh	312.9(1)	291.6(1)	0.932	24.73

highest pressure reached in this study was 30 GPa. Diffraction spectra were evaluated with the computer programs EDXPowd and XPOWDER [16].

3. Results

Diffraction patterns of the HgSn alloy at ambient pressure contain diffraction peaks only from the sh-*hP*1 phase, because the Hg-rich phase is liquid. The crystallisation process of the liquid phase with increasing pressure is difficult to record on the EDX spectra, because large grains are formed during solidification, leading to strong effects of texture. However, diffraction patterns of well-crystalline phases of the alloy are recorded on compression above 5 GPa and on decompression down to 2.6 GPa.

Selected patterns of HgSn at different pressures up to ∼30 GPa in one run are shown in figure 1. The ambient-pressure sh-*hP*1 phase exists up to 14 GPa. At higher pressures it transforms to the bct-Sn-II type phase. Another crystalline phase recorded together with the sh-*hP*1 phase (figure 1, $P = 9.4$ GPa) was identified as a rhombohedral *hR*1 phase of α-Hg type. However, this phase is not a pure α-Hg, which is stable at pressure below 3.7 GPa and transforms at this pressure to bct-Hg. The rhombohedral phase in HgSn alloy is apparently a solid solution of Sn in α-Hg and is referred to further as *hR*1-(Hg).

The phase *hR*1-(Hg) remains stable up to ∼30 GPa, the highest pressure reached in this study. At pressures higher than 15 GPa, this phase coexists with the bct Sn-rich phase. The relative intensities of the reflections from the bct-*tI*2 phase slightly increase with increasing pressure at the expense of the *hR*1-(Hg) phase. This indicates that the amount of the phases in the sample and the phase composition are pressure dependent. On decompression, the reverse transformations are observed, and the *hR*1-(Hg) phase was recorded down to 2.6 GPa in coexistence with the sh-*hP*1 phase (figure 1, upper pattern). On complete pressure release, only the crystalline sh-*hP*1 phase was recorded, implying the recovery of the liquid Hg-rich phase. Table 1 lists the structural characteristics of the phases observed in the diffraction patterns shown in figure 1.

A diffraction pattern of HgSn at 11.3 GPa obtained in another run is shown in figure 2. Two phases are identified: sh-*hP*1 and *hR*1-(Hg) with lattice parameters given in table 2. Observed and calculated d-spacings and intensities are listed with excellent agreement in d-spacings and satisfactory agreement in intensities indicating some texture effects.

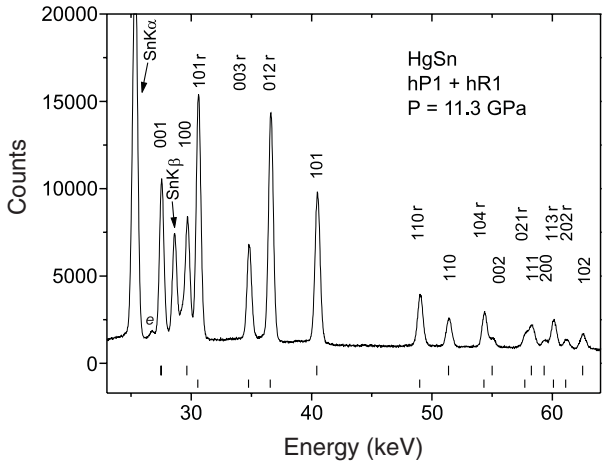

Figure 2. EDXD pattern of the HgSn alloy at pressure $P = 11.3$ GPa collected with $2\theta = 9.03°$ ($Ed = 7875$ keV pm). The alloy contains two phases: the Sn-rich $hP1$-sh phase and the Hg-rich $hR1$-(Hg) phase; indices are given as hkl and hkl_r, respectively. Tick marks below the pattern show the calculated peak positions for each phase listed in table 2. Fluorescence peaks from Sn are marked by arrows; 'e' denotes an escape peak.

Table 2. Observed and calculated d-spacings and diffraction intensities of the HgSn alloy at $P = 11.3$ GPa for the two-phase mixture $hP1$ and $hR1$ in the pattern in figure 2. The intensities are calculated with a sample thickness of 40 μm, for randomly disordered phases based on Sn and Hg, with addition of 10 at.% Hg or Sn, respectively.

		$hP1$, $P6/mmm$ $a = 306.49(8)$ pm $c = 286.20(9)$ pm				$hR1$, $R\bar{3}m$ $a = 321.46(2)$ pm $c = 678.68(7)$ pm			
d_{obs} (pm)	I_{obs}	d_{calc} (pm)	δd ($d_{calc} - d_{obs}$)	hkl	I_{calc}	d_{calc} (pm)	δd ($d_{calc} - d_{obs}$)	hkl	I_{calc}
286.05	60	286.20	0.15	001	41	—	—	—	—
265.37	50	265.43	0.06	100	100	—	—	—	—
257.46	100	—	—	—	—	257.57	0.11	101	100
226.26	37	—	—	—	—	226.23	−0.03	003	24
215.17	96	—	—	—	—	215.23	0.06	012	61
194.57	67	194.62	0.05	101	45	—	—	—	—
160.68	24	—	—	—	—	160.73	0.05	110	18
153.22	13	153.25	0.03	110	8	—	—	—	
144.90	15	—	—	—	—	144.88	−0.02	104	11
143.14	4	143.10	−0.04	002	2	—	—	—	—
136.41	5	—	—	—	—	136.36	−0.05	021	8
135.14	12	135.10	−0.04	111	9	—	—	—	—
132.71	4	132.71	0.00	200	4	—	—	—	—
131.00	14	—	—	—	—	131.03	0.03	113	12
128.78	5	—	—	—	—	128.78	0.00	202	5
125.93	7	125.96	0.03	102	6	—	—	—	—

Atomic volumes and axial ratios for the phases obtained in this study are shown in figure 3. The data from the previous study on the alloy $Hg_{15}Sn_{85}$ [3] are also included for the Sn-rich bct-Sn-II type phase. An additional phase observed in the alloy $Hg_{15}Sn_{85}$ in a small amount was previously assigned as a tetragonal distortion of fcc. However, in the light of the present

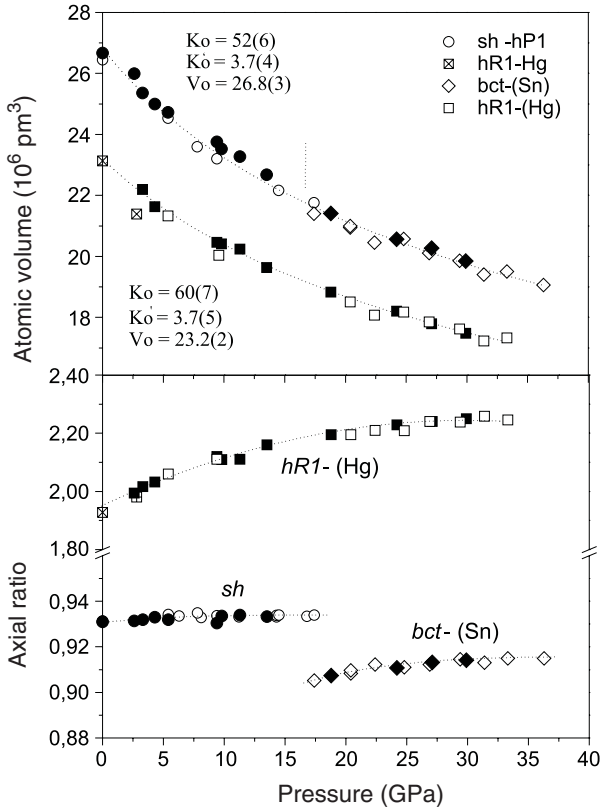

Figure 3. The pressure dependence of the atomic volumes (upper plot) and of axial ratios c/a (lower plot) for the phases in the Hg–Sn alloys: sh-$hP1$, bct-(Sn) and $hR1$-(Hg). Data on the HgSn alloy from the present study are shown by solid symbols. Data on the $Hg_{15}Sn_{85}$ alloy from the previous study [3] are shown by open symbols. Data for pure Hg [7] are shown by crossed symbols. The P–V data are fitted by EOS, shown by dotted curves, with respective parameters K_o, K_o', V_o indicated in the upper plot. The Sn-rich phases sh-$hP1$ and bct-(Sn) are fitted with common EOS; the transition pressure between these phases is indicated by the vertical line. The curves connecting the experimental data of c/a versus P are guides to the eye.

results, the data on this phase are re-evaluated with a rhombohedral distortion of the fcc cell, and are also shown in figure 3. Taking into account previous data [3], we conclude that the $hR1$-(Hg) phase remains stable up to at least 36 GPa.

The experimental data on atomic volumes in figure 3 are fitted by Murnaghan equations of state [17] for both Sn-rich phases sh and bct and for the Hg-rich $hR1$ phase. These fits should be considered as qualitative estimations taking into account that for both phases small changes in composition with pressure are possible. The Sn-rich phases sh and bct are fitted with one equation of state because the volume change at the transition between these phases is found to be relatively small ($\leqslant 1.1\%$) [10]. The fit parameters $K_o = 52(6)$ GPa and $K_o' = 3.7(4)$ are in agreement with previously observed values 59(1) GPa and 3.9(1), respectively [10], and $V_o = 26.8(3) \times 10^6$ pm^3 corresponds to the atomic volume of sh-$hP1$ at ambient pressure [9]. For the $hR1$-(Hg) phase, the determined fit parameters are $K_o = 60(7)$ GPa, $K_o' = 3.7(5)$ and $V_o = 23.2(2) \times 10^6$ pm^3. These values are comparable with the compressible moduli of hcp-Hg $K_o = 60(3)$ and $K_o' = 6.1(1)$, respectively [7], and with $V_o = 23.13 \times 10^6$ pm^3 for pure α-Hg [4].

There is an important consequence from the volume–pressure relations presented in figure 3 that indicate no significant change in phase compositions with pressure. The atomic volumes of Sn-rich and Hg-rich phases in the pressure range studied are ranged between volumes of pure components, which corresponds to the known Vegard's law for solid solutions, assuming approximately 10 at.% of solubility on the both component sides. The solubility limits for both components are discussed below (section 4).

Atomic volumes for both Hg-rich and Sn-rich high-pressure phases extrapolated to the ambient pressure allow us to estimate the sample composition. In accordance with Vegard's law, an average atomic volume for the equiatomic alloy is one half of the sum of volumes for pure components. Taking ambient-pressure atomic volumes for Hg and Sn as 23.4 and 27.1×10^6 pm^3, respectively [4], one obtains for the equiatomic alloy $V = 25.25 \times 10^6$ pm^3. This value is very close to the average volume $V_o = 25.0 \times 10^6$ pm^3 defined as one half of the sum of values V_o obtained from a EOS fits for the Hg-rich and Sn-rich phases in our studies. So far the composition of both phases is assumed to be about 10 at.%; the average volume V_o for the phases in the sample corresponds within experimental error to the alloy composition 50/50.

Axial ratios for both Sn-rich phases sh and bct display very slight increase with pressure in agreement with previous observations [3, 10]. For the sh-$hP1$ phase, c/a increases from 0.931 to 0.934 in the pressure range from ambient to $\sim$15 GPa. For the bct-$tI2$ phase, c/a increases from 0.907 to 0.914 as the pressure increases from 13 to 30 GPa. In contrast to these Sn-rich phases, the $hR1$-(Hg) phase shows a very strong anisotropy in compression along the a and c axes. The axial ratio for the hexagonal cell increases from $c/a = 1.99$ to 2.25 in the pressure range from 2.6 to 29.9 GPa, indicating a low compressibility along the c-axis compared to that of the a-axis. The rhombohedral angle for the corresponding rhombohedral cell decreases in this pressure range from 69.2° to 63.9° as shown in figure 4, revealing the trend toward the fcc structure where the rhombohedral angle is 60°. The interatomic distances in the $hR1$-(Hg) phase become closer under pressure, as shown in figure 4, with the trend to increase the coordination number from 6 + 6 to 12. However, the observed behaviour of the $hR1$-(Hg) phase with increasing pressure indicates that the transition from the rhombohedral phase to fcc is expected to be discontinuous with a jump in the axial ratio and lattice parameters. Studies at higher pressures are necessary to check this suggestion.

4. Discussion

4.1. The Hg-rich phase

The observation of the rhombohedral α-Hg type phase in the Hg–Sn alloy system in a wide range of pressure from 2.6 to 30 GPa raises the question about the origin of the stability of this phase in pure Hg and in Hg alloyed with Sn. The crystal structure energy is usually considered to consist of an electrostatic term and a band structure contribution, where the former favours high symmetry structures and the latter accounts for distortions of the high symmetry structures [18, 19]. The stability of the α-Hg structure with a rhombohedrally distorted fcc cell is related to the Hume-Rothery effect in the Cu–Zn and other brass-like alloy systems. The crystal structure and phase sequences in these alloys along the composition are controlled by the average number of valence electrons per atom, or electron concentration, that was explained within the concept of Brillouin zone (BZ)–Fermi sphere (FS) interactions [20, 21].

In the nearly-free electron approximation, energy gaps evolve in the electron dispersion relation at the BZ boundaries due to the interaction of the free electrons with the periodic lattice potential. The energy of electrons with k-vector close to a BZ boundary is lowered

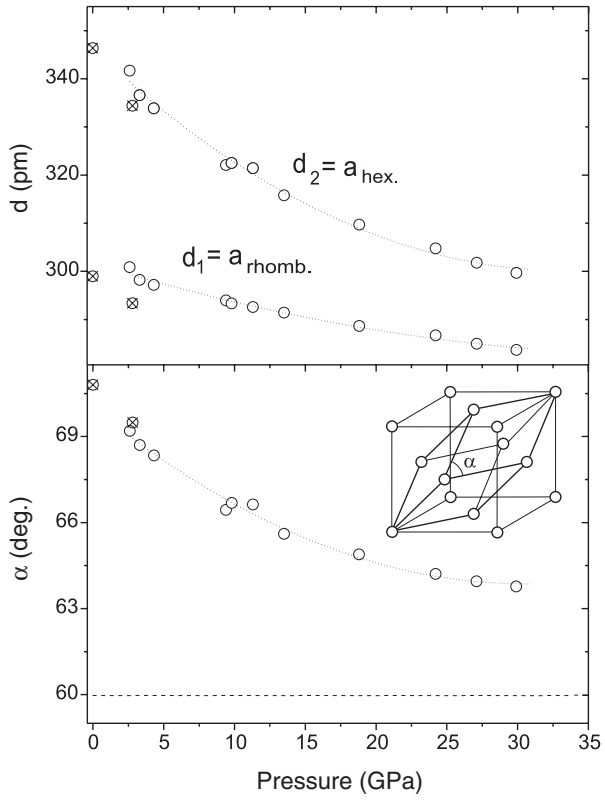

Figure 4. Variations of the interatomic distances (upper plot) and the rhombohedral angle (lower plot) with pressure for the *hR*1-(Hg) phase in the HgSn alloy from the present study (open symbols). Data for pure Hg [7] are shown by crossed symbols. The dotted curves connecting the experimental data are guides to the eye. The rhombohedral angle 60° corresponding to fcc is indicated by the horizontal dashed line. The relation between fcc and primitive rhombohedral cell *hR*1 is shown in the inset.

and the total electron (band structure) energy is minimised if the FS is tightly enclosed by BZ boundaries, i.e. $(1/2)q_{hkl} \leqslant k_{\mathrm{F}}$.

The α-Hg phase in pure mercury. The divalent metal Hg crystallises in a rhombohedral structure, which can be considered as a distortion of the fcc cell by contraction along one of the [111] directions and corresponding elongation along the other [111]-type directions to keep the cell volume constant. The degree of the distortion and hence the particular value of c/a for the hexagonal cell can be understood by considering the configuration of the BZ and the FS for the hypothetical fcc and the real *hR*1-Hg cells with the same volume, as shown in figure 5. For the BZ of fcc, there are eight planes $\{111\}$ intersecting the FS and six planes $\{200\}$ lying outside but close to the FS. By a rhombohedral distortion of the fcc cell into *hR*1-Hg, the planes $\{200\}_{\mathrm{fcc}}$ rename to $\{012\}$ and the set of planes $\{111\}_{\mathrm{fcc}}$ splits into two sets of $\{101\}$ and $\{003\}$ in such a way that the latter moves outside the FS and became equidistant to $\{012\}$. This distortion leads to a decrease in the number of planes intersecting the FS (six planes $\{101\}$) and to an increase in the number of planes lying outside the FS in close contact (six planes $\{012\}$ and two planes $\{003\}$). Assuming the respective reciprocal vectors to be equidistant ($q_{012} = q_{003}$), one can estimate the axial ratio for the hexagonal cell to

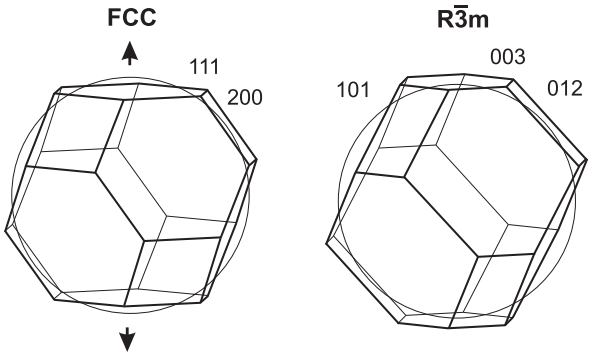

Figure 5. BZs for the fcc and *hR*1-Hg structures illustrating the relation between these structures and the deformation mechanism with the elongation of one of the [111] axes of the reciprocal lattice, as shown by arrows, and respective contraction of the others. The circles represent the FS corresponding to k_F for $z = 2$ electron/atom.

be $c/a = \sqrt{15}/2 = 1.936$ as is experimentally found for α-Hg. Thus, the trend to form a BZ containing more planes placed close to the FS with equidistant vectors accounts for the rhombohedral distortion of α-Hg.

The α-(Hg) phase in the solid solution with Sn. Similar considerations allow us to understand the stabilisation of the α-Hg phase by alloying with metals of higher valency, such as In or Sn, and to assert the limiting composition ranges for the α-(Hg) solid solutions. This limit can be estimated from the condition that the FS touches the BZ planes $(1/2)q_{012} = k_F$, where $k_F = (3\pi^2 z/V_{at})^{1/3}$. Assuming $c/a = \sqrt{15}/2$ as for pure α-Hg, this estimation gives $z = 2.17$, which can be obtained by the alloying of Hg with 17 at.% of a trivalent metal or with 8.5 at.% of a tetravalent metal. This estimation of ranges of stability for α-(Hg) is confirmed in the Hg–In alloy system at ambient pressure, where the solubility of In in α-(Hg) extends up to 16 at.% [8]. In the case of the Hg–Sn alloy system studied under pressure, the alloying of α-(Hg) with Sn should be asserted with the upper limit of 8–10 at.% Sn. These estimations are qualitative and further experiments are necessary to confirm the conclusions based on the model of FS–BZ interactions.

In pure Hg, the *hR*1 phase is stable up to 3.7 GPa and transforms at higher pressure to a β-Hg, bct-*tI*2 phase [6, 7]. The latter could be considered as a tetragonal distortion of an fcc structure with strong contraction along one of the [002]-type directions. The axial ratio of β-Hg for the body-centred cell has a specific value of $c/a = 0.705$, which is close to $1/\sqrt{2}$. At this value of c/a the coordination number is $N = 10$ (with nearly equal interatomic distances). On the other hand, at this c/a there is a special fit of the BZ to the FS as $(1/2)q_{101} = k_F$. Thus, the valence band contribution plays a significant role for stability of β-Hg phase under pressure. This phase is also stabilised at ambient pressure by the substitution of Hg with the isoelectronic element Cd over a wide range of composition [8]. Comparing alloying effects on stability of Hg polymorphs, one can conclude that the divalent Cd stabilises β-Hg, whereas the trivalent/tetravalent elements In/Sn stabilise α-Hg, in agreement with the free-electron model of BZ–FS interactions.

4.2. The Sn-rich phases

The results on the Sn-rich phases in the HgSn alloy in the present study are discussed together with the results on alloys $Hg_{10}Sn_{90}$ and $Hg_{15}Sn_{85}$ reported in previous studies [10, 3]. The

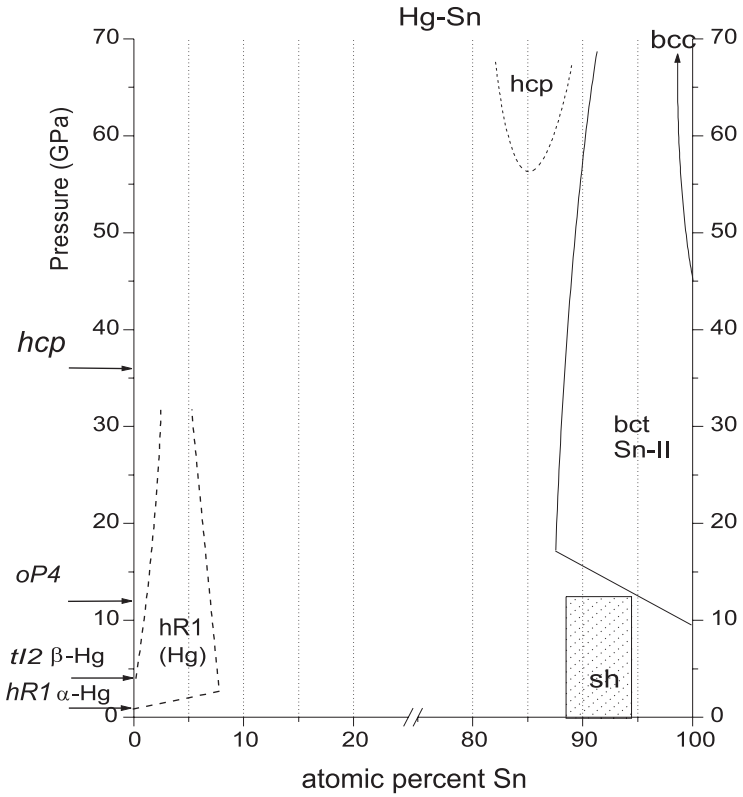

Figure 6. Proposed P–x diagram of phase regions for the Hg–Sn alloy system on the Hg and Sn sides. The phases and transition pressures for pure Hg and Sn are taken from [6, 7] and [5]. The phase regions on the Sn-rich part are based on data from [3, 10].

ambient-pressure phase $HgSn_9$, sh-$hP1$, transforms under pressure above 15 GPa into a bct-$tI2$ phase, which is a solid solution of Hg in the high-pressure phase of Sn. While in pure Sn the bct phase transforms to bcc at ∼45 GPa [5], the addition of Hg was found to stabilise the bct phase to a higher pressure of ∼65 GPa [10]. The appearance of new diffraction peaks at pressures above ∼55 GPa was treated previously as an orthorhombic distortion of the bct phase [10], however one additional intermediate phase (hcp) has been identified later [3], in similarity with the results on the $In_{20}Sn_{80}$ alloy with the ambient-pressure sh-$hP1$ phase [22]. The extension of solid solution based on bct-Sn-II does not exceed 10 at.% Hg, and the range of solubility decreases slightly under pressure above 50 GPa where a new intermediate hcp phase appears in addition to the bct-(Sn) phase. The alloy composition where this hcp phase appears should be assigned with approximately 13–15 at.% Hg as reported in [3] and shown in figure 6. The Sn-rich part of the phase diagrams for the Hg–Sn and In-Sn alloy systems are similar [3] if one estimates phase regions in the valence electron concentration taking into account for Hg $z = 2$ and for In $z = 3$.

The Sn-rich phases sh-$hP1$ and bct-$tI2$ are characterized by special values of axial ratio as was discussed in previous works (see [22, 10] and references therein). The c/a ratio for the $hP1$ structure in all alloys so far investigated and also for the elements Si and Ge has been found to lie between 0.92 and 0.95. This is related to a special balance of real and reciprocal lattice contributions in the Ewald sum when $c/a \approx c^*/a^*$, resulting in the axial ratio $(\sqrt{3}/2)^{1/2} = 0.931$ [23]. The sh phase in a $Ga_{20}Sn_{80}$ alloy recently synthesised under

pressure has a similar $c/a = 0.928$ [3]. On the other hand, all existing sh phases in group IV elements and/or in their alloys have a certain value of the valence electron to atom ratio ranging from 3.7 to 4.0, which indicates a basic electronic origin for their stability.

For the bct-$tI2$ phases in Sn alloyed with Hg, the c/a value varies with pressure very slightly from 0.907 to 0.920 with the trend to saturate at the latter value under pressure above ~40 GPa [10]. The c/a ratio for the bct-$tI2$ phase is determined by the alloy electron concentration and is accounted for by BZ–FS interactions assuming the close contact of k_F with the BZ planes $\{200\}$. This model allows us to estimate the upper value of c/a for the $tI2$ structure from the condition $(1/2)q_{200} \leqslant k_F$ or $2\pi/a_t \leqslant k_F$, which gives $c/a \leqslant (3/4\pi)z$. From these estimations, for $z = 4$ the axial ratio should be $c/a \leqslant 0.96$ as was found experimentally for Sn and InBi [5, 24]. For $z = 3.8$, the axial ratio should be $c/a \leqslant 0.91$, in good agreement with the experimentally observed upper value of ~0.92 for the bct phase with the composition $Hg_{10}Sn_{90}$ in the present and previous [3, 10] studies.

5. Conclusions

In the Hg–Sn alloy system under ambient conditions, there are very limited ranges of terminal solubility and only one intermediate phase of composition $HgSn_9$. The constituent elements Hg and Sn have a small difference in atomic size and electronegativity, so one can expect extended ranges of solid solutions under pressure. In addition, both constituents are known to transform under pressure to similar body-centred tetragonal structures, $tI2$, which differ only slightly in $c/a = 0.707$ for β-Hg at 77 K (quenched from pressure) [4] and $c/a = 0.91$ for bct-Sn at 10 GPa [5]. However, the results of the present work show that the formation of a Sn solid solution in Hg stabilises the α-Hg rhombohedral structure, which exists at least up to 30 GPa. Thus, both components in the Hg–Sn alloy system form under pressure (above 15 GPa) solid solutions based on $hR1$-Hg and $tI2$-Sn, respectively, within composition ranges extended approximately to 10 at.% on both sides. Results obtained for the Hg–Sn alloys demonstrate that phase formation and stability in this system under compression are controlled primarily by factors originating from valence electron effects. This behaviour of the Hg–Sn alloys with respect to phase formation correlates with the concept of FS–BZ interaction and is related to the stability of the Hume-Rothery phases in the brass-like alloys.

The existence of the $hR1$-(Hg) phase in the wide range of pressures from ~3 to 30 GPa provides a unique possibility to study the behaviour of this distorted structure at strong compression. The changes in the rhombohedral structure with compression are found to cause an increase in the coordination number from 6 + 6 to 12 with the trend to approach the fcc phase. These changes follow a possible shift in the energy balance between electronic band structure and electrostatic contributions, when the former is dominant at moderate pressures and the latter becomes more significant at very strong compression.

References

[1] Ponyatovskii E G and Degtyareva V F 1989 *High Pressure Res.* **1** 163
[2] Degtyareva V F 2002 *Acta Phys. Pol.* A **101** 675
[3] Degtyareva O, Degtyareva V F, Porsch F and Holzapfel W B 2002 *J. Phys.: Condens. Matter* **14** 389
[4] Pearson W B 1972 *The Crystal Chemistry and Physics of Metals and Alloys* (New York: Wiley–Interscience)
[5] Olijnyk H and Holzapfel W B 1984 *J. Physique Coll.* **45** C8 153
[6] Schulte O and Holzapfel W B 1993 *Phys. Rev.* B **48** 14009
[7] Schulte O and Holzapfel W B 1996 *Phys. Rev.* B **53** 569
Schulte O 1994 *Thesis* Paderborn University
[8] Massalsky T B (ed) 1996 *Binary Alloy Phase Diagrams* (Metals Park, OH: American Society for Metals)

[9] Che G C, Ellner M and Schubert K 1991 *J. Mater. Sci.* **26** 2417
[10] Degtyareva V F, Degtyareva O, Winzenick M and Holzapfel W B 1999 *Phys. Rev.* B **59** 6058
[11] Syassen K and Holzapfel W B 1975 *Europhys. Conf. Abstr.* A **1** 75
[12] Grosshans W A, Düsing E F and Holzapfel W B 1984 *High Temp.–High Pressure* **16** 539
[13] Otto J W 1997 *Nucl. Instrum. Methods Phys. Res.* A **384** 552
[14] Forman R A, Piermarini G J, Barnett J D and Block S 1972 *Science* **176** 284
[15] Mao H K, Bell P M, Shaner J W and Steinberg D J 1978 *J. Appl. Phys.* **49** 3276
[16] Porsch F 1995 *EDXPowd and XPOWDER—Programs for Evaluation of EDXD Spectra* RTI, Paderborn, Germany
[17] Murnaghan F D 1967 *Finite Deformation of an Elastic Solid* (New York: Dover)
[18] Heine V and Weaire D 1970 *Solid State Physics* vol 24 (New York: Academic)
[19] Harrison W A 1966 *Pseudopotentials in the Theory of Metals* (New York: Benjamin)
[20] Mott N F and Jones H 1936 *The Theory of the Properties of Metals and Alloys* (Oxford: Oxford University Press)
[21] Jones H 1962 *The Theory of Brillouin Zones and Electron States in Crystals* (Amsterdam: North-Holland)
[22] Degtyareva V F, Degtyareva O, Holzapfel W B and Takemura K 2000 *Phys. Rev.* B **61** 5823
[23] Weaire D and Williams A R 1969 *Phil. Mag.* **19** 1105
[24] Degtyareva V F, Winzenick M and Holzapfel W B 1998 *Phys. Rev.* B **57** 4975